SPATIALLY INDIRECT PHOTOLUMINESCENCE FROM InAs/AlSb HETEROSTRUCTURES

F. Fuchs, J. Schmitz, J.D. Ralston, and P. Koidl
Fraunhofer Institut für Angewandte Festkörperphysik,
Tullastrasse 72, D-79108 Freiburg, Germany

R. Heitz and A. Hoffmann
Institut für Festkörperphysik, TU Berlin,
Hardenbergstr. 36, D-10623 Berlin, Germany

(Received 22 August 1994)

We present a Fourier transform photoluminescence study of InAs/AlSb type II heterostructures, spanning the mid infrared 1 µm - 12 µm wavelength range. The investigated samples consist of single-, double-, and multi-quantum wells, grown on GaAs substrates by molecular beam epitaxy, with different buffer layer structures for strain accommodation. The photoluminescence intensity is found to be very sensitive to the detailed structure of the underlying buffer sequence. Calorimetric measurements of the absorbance at 500 mK shows the weak spatially indirect transitions superimposed onto the spatially direct absorbance. Very wide quantum wells (100 nm and 200 nm) exhibit spatially direct as well as spatially indirect photoluminescence. Polarization resolved photoluminescence of the spatially indirect transitions allow the contributions of the normal (AlSb on InAs) and the inverted (InAs on AlSb) interface to be separated.

1. Introduction

Heterostructures based on the InAs/AlSb/GaSb material system are attracting increasing interest because of their very promising technological applications [1] and unique physical properties. The valence band maximum of the AlSb barrier is located about 100 meV above the valence band maximum of InAs, whereas the conduction band minimum resides in the InAs layers. The conduction band offset [2] has a value of 1.95 eV at the Γ-point providing excellent electronic confinement. This type II band alignment leads to a spatial separation of electrons and holes. High electron concentrations [3], typically on the order of 10^{12} cm^{-2} with mobilities [4] exceeding 10^5 cm^2/Vs are found in InAs/AlSb quantum wells even in the absence of intentional doping. The main carrier contribution is shown to originate from the AlSb barrier material [5].

Recently, it has been suggested [6] that the cation-on-anion antisite defect establishes a deep level in the AlSb barrier, which should be responsible for the dominant contribution of the observed remote n-doping of the InAs channels, which has been supported by a study of the mid infrared emission of single quantum wells (SQW's) [14]. The InAs/AlSb interface can in principle be driven to be AlAs - or InSb-like via the epitaxial growth sequence [4]. Besides far infrared magneto-optical transport studies [7,8], Raman investigations have been published focusing on heterostructure interface properties [9-11]. Photoluminescence (PL) in the near infrared on InAs/AlSb short period superlattices has also been [12,13] reported.

In the present work, the PL of a multi-quantum well (MQW) and two double quantum wells (DQWs) will be compared with the absorbance measured via calorimetric techniques. Furthermore, very wide quantum wells were investigated (100 nm and 200 nm). These wide quantum wells show both the spatially *direct* PL-transitions of the InAs well and the spatially *indirect* radiative recombination of electrons and holes across the type II hetero-interface. Polarization resolved measurements of the spatially indirect transitions allow us to separate the contributions of the normal (AlSb on InAs) and the inverted (InAs on AlSb) interface.

2. Experimental

The samples were grown by solid-source molecular-

0749-6036/94/050035+06 $08.00/0 © 1994 Academic Press Limited

beam epitaxy (MBE) on {100} GaAs substrates. The arsenic flux was controlled by a valved-cracker effusion cell, which facilitates the reduction of the arsenic background pressure during growth of the antimonides by up to three orders of magnitude as compared to conventional arsenic effusion cells [15,16]. In the MQWs and DQWs investigated here, a 1000 nm thick relaxed AlSb (GaSb) buffer was grown for accommodation of the lattice constant misfit. One SQW also had a GaSb/AlSb superlattice grown on the AlSb buffer. Then the InAs/AlSb heterostructures were deposited. The shutter sequence was programmed such as to promote InSb-like interfaces [4], which was confirmed via Raman measurements [11,15]. Finally, the structures were capped with 10 nm of GaSb to prevent degradation. The very wide InAs layers of 100 nm and 200 nm thickness, respectively, were embedded in 40 nm AlSb barriers grown on a GaSb buffer.

The optical measurements were carried out with a Fourier transform spectrometer, using double modulation techniques as described elsewhere [17]. An InSb photodiode operating at 77 K was used to detect the PL. The samples were positioned in a He exchange gas cryostat. Optical excitation was accomplished either with visible radiation from an argon laser (2.54 eV or 2.71 eV) or with the IR radiation of a YAG:Nd laser (0.94 eV or 1.17 eV). In the Fourier transform photoluminescence excitation (FTPLE) experiment the broad band emission of a glowbar source, after traversing the interferometer, excited the PL of the sample. More details of the FTPLE technique can be found in Refs. [18] and [19]. The calorimetric absorption spectroscopy (CAS) experiments were performed using a ^{3}He/^{4}He-dilution refrigerator. The spectra were taken by measuring the sample temperature in dependence of the excitation wavelength, using a dispersive spectrometer. Typical sample temperatures in the present CAS experiments were around 500 mK. More details can be found in Ref. [20].

3. Results and Discussion

The PL intensity is found to be very sensitive to the structure of the buffer sequence, as shown in Fig. 1. Spectrum (a) has been obtained from a 5 nm InAs SQW grown on a GaSb/AlSb short period SL on top of an AlSb buffer. Spectrum (b) corresponds to a 7.5 nm SQW grown on top of a GaSb buffer. Spectrum (c) is observed from a double quantum well (DQW), where the two 7.5 nm InAs channels were separated by an AlSb barrier of 7.5 nm width. Spectrum (d) has been obtained from a 7.5 nm InAs DQW sample grown on an AlSb buffer with no GaSb layers inserted. The spectra are corrected for the system response and scaling factors are indicated in the figure.

In Fig. 1 we observe a strong anti-correlation of the PL intensity of the InAs quantum well structure with the PL intensity of the buffer layers. Strong radiative recombination from the short period SL is observed in the near IR in spectrum (a), where the intensity of the InAs SQW is very weak. In contrast, the DQW structure grown on a thick AlSb buffer (d), which does not show PL in the near IR, exhibits very strong emission from the InAs QW's. The intensity variation of the QW emission covers about two orders of magnitude. The sample with the most intense PL (d) exhibits an additional transition around 10 μm, with comparable intensity to the QW emission. The origin is not known. The cut-off at 650 cm^{-1}of this spectrum is given by the $Hg_{1-x}Cd_xTe$ photo-conductor which has been used for detection of the low energy part. In the following we concentrate on the intensity dependence of spectra (a) to (d).

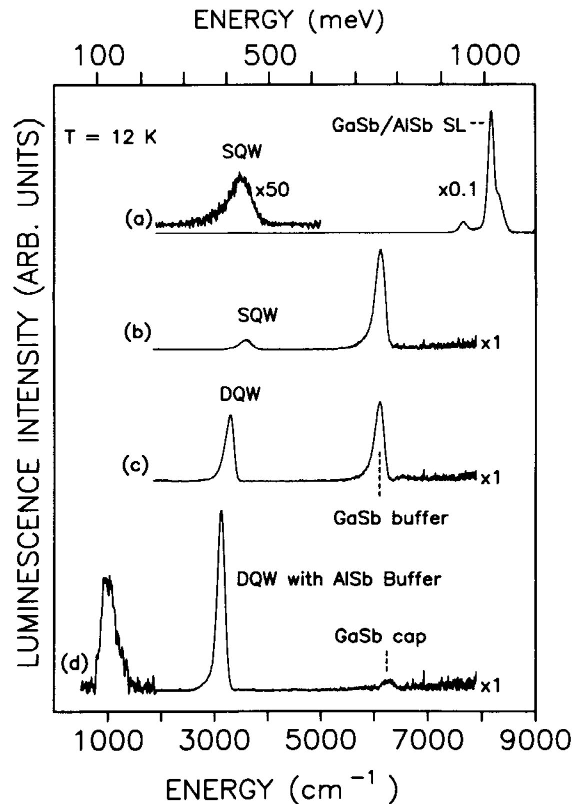

Fig. 1. Evolution of the PL intensity with change of the buffer structure. (a) 5 nm InAs/AlSb single quantum well (SQW) grown with a GaSb/AlSb short period SL on top of a AlSb buffer, (b) 7.5 nm SQW with GaSb buffer, (c) 7.5 nm double quantum well (DQW) with GaSb buffer, (d) 7.5 nm DQW with AlSb buffer, using GaSb only for the cap layer. The spectra are corrected for the system response

3.1. Hole Generation, Diffusion, and Trapping

From the spectra shown in Fig. 1 it is evident that GaSb

layers in the buffer sequence introduce a competing recombination channel due to the type II band alignment of the materials. Only sharp interfaces provide finite spatial overlap of the electron and hole wavefunctions to enable radiative recombination involving the InAs QW's. Due to electrostatic band bending there is some localization of the holes at the hetero-interfaces. However, the photogenerated holes can relax energetically into the GaSb layers, where the valence band is located about 0.35 eV [2] *above* the valence band maximum of AlSb. This is confirmed by the intensity enhancement by a factor of 5 observed with a DQW compared to a SQW, where the hole-confinement between the two InAs channels prevents diffusion away from the hetero-interfaces. Finally, the most intense PL is observed from the sample containing no GaSb buffer layers (d). Thus, we conclude, the PL results can be consistently understood in terms of hole generation, diffusion and capture, which are all strongly influenced by the presence of GaSb layers in the buffer sequence.

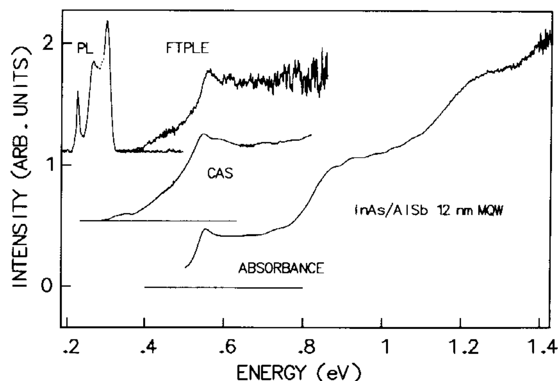

Fig. 2. PL and absorbance data of an InAs/AlSb MQW consisting of 100 QWs of 12 nm width, separated by 10 nm wide barriers. The absorbance has been measured via FTPLE, CAS and conventional transmission. The PL has been excited with 2.7 μm wavelength radiation.

3.2. Calorimetric Measurements

In Fig. 2 the optical data of an InAs/AlSb MQW sample are collected. The heterostructure consists of 100 periods of 12 nm wide InAs QWs separated by 10 nm wide AlSb barriers, such that coupling between the individual QW's is not significant. This sample allows to measure the absorbance via conventional transmission in the spectral region above 4000 cm^{-1}. Since the refractive index of the heterostructure is higher as compared to the GaAs substrate, the heterostructure induces multiple reflection modulation of the transmission according to the optical thickness of about 2 μm. While the strong spatially direct absorption can be measured by transmission spectroscopy, the multiple reflection of the epitaxial layer obscures the weak absorbance arising from the spatially indirect transitions across the heterointerface. This contribution, however, can be measured either with CAS (Fig. (2)) or, if the PL intensity is sufficiently intense, via FTPLE. The PL shows up at the onset of the spatially indirect absorbance. The step-like shape of the absorbance reflects the subband structure of the electronic system. At the low-energy side of these steps the spatially indirect contributions start at lower energies corresponding to the expected value of the valence band offset (VBO) of 100 meV.

In Fig. 3 PL and CAS spectra of two DQWs are shown. The absorbance of these samples was not measurable via conventional transmission experiments. The samples are nominally identical. Only the thickness of the InSb-like interfaces has been tried to vary between 2 and 3 MLs. The CAS spectra of the two samples are identical within the experimental error. However, the PL of the sample with 3 ML InSb interface is red-shifted below the low-energy detection limit of the InSb photodiode at 1600 cm^{-1}. This PL spectrum has been recorded with a MCT photoconductor, resulting in enhanced noise contributions. The red-shift of the PL can be explained with two models.

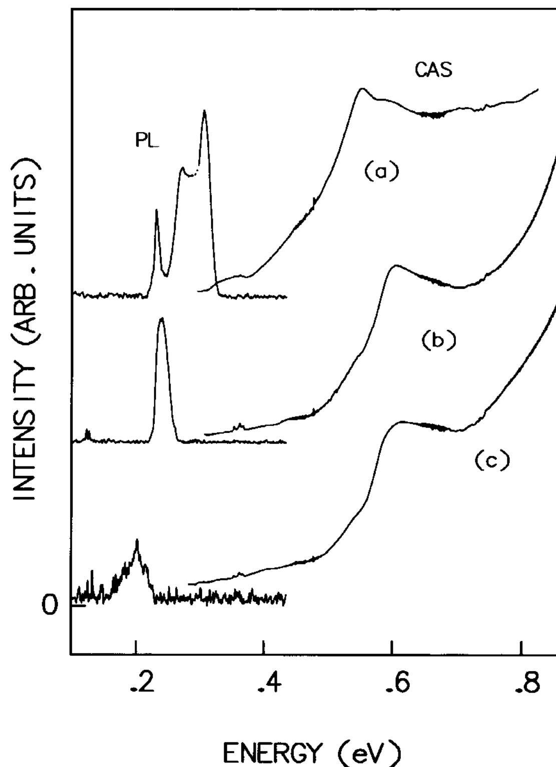

Fig. 3. PL and calorimetric absorbance of a 12 nm MQW (a) and two 7.5 nm DQWs. The DQWs were growth with intentionally 2ML (b) or 3 ML (c) thick InSb-like IFs, respectively.

(i) The growth of 3 ML InSb results in the creation of additional deep defects at the heterointerface. (ii) Growth of two or three ML InSb establishes additional hole confinement according the energetically higher valence-band maximum of InSb compared to AlSb. Similar observations have been made recently with short period InAs/AlSb SLs emitting in the near infrared [13]. In these experiments the transition energy of the sample with InSb-like interfaces was lowered by 96 meV as compared to the sample with AlAs-like IFs. This observation supports that the growth of InSb monolayers establishes hole confinement, leading to the observed red-shift.

3.3. Spatially indirect and direct Transitions

In this section, we consider very wide InAs layers with a thickness of 100 nm and 200 nm sandwiched between 40 nm thick AlSb barriers grown on a 1000 nm GaSb buffer layer. In such wide QW's we have to expect the formation of triangular shaped electron channels at the top and bottom hetero-interfaces due to the electrostatic band bending. Furthermore, due to comparable dimensions of the layer thickness and hole diffusion length, this type of samples will also exhibit bulk-like properties.

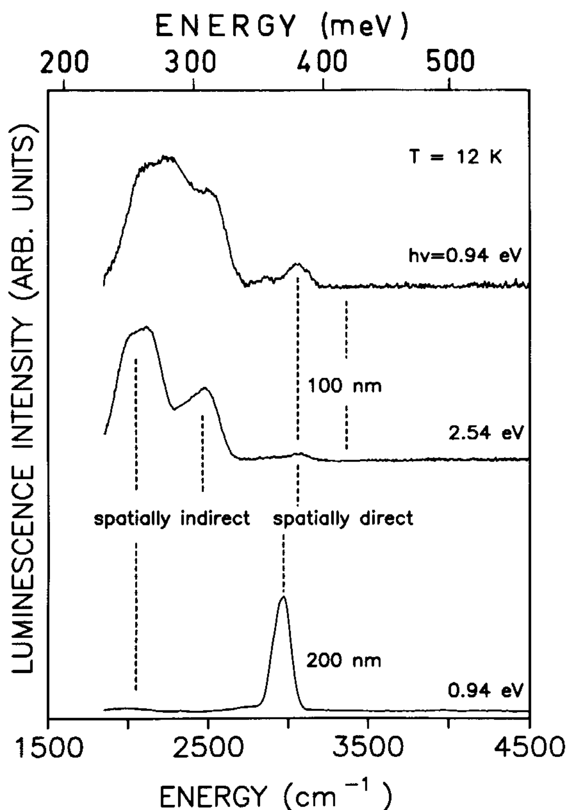

Fig. 4. Spatially direct and indirect PL of very wide InAs quantum wells.

The spectra obtained from these two very wide InAs QW's are shown in Fig. 4. These samples do not exhibit any detectable signal at transition energies below 220 meV. Besides a weak feature at 250 meV, the spectrum of the 200 nm layer (bottom) consists of one single line. This line is located at an energy of 366 meV in excellent agreement with the prediction of an InAs band gap [8] of 357 meV in the case of biaxial tensile strain due to growth on GaSb. In contrast, the 100 nm layer exhibits only a weak transition near the same spectral position of the InAs band gap, while two broad bands at lower transition energy become dominant. These bands are separated from the transition at 366 meV by energies of 74 and 124 meV. The relative intensity of the two bands is altered when the excitation wavelength is changed. For visible excitation the high energy component is weakened, whereas the spectral shape of the individual components is not affected significantly.

Due to band bending in the 200 nm wide layer, there will be a weak confinement attracting the photo-generated holes towards the center of the InAs layer, thus preventing them from diffusing towards the AlSb layers. This explains the strong PL intensity at the energy expected for the bulk transition. Therefore, the high energy transition at 366 meV is due to spatially *direct* recombination in the bulk-like InAs layer. In the 100 nm layer the hole confinement is weakened, since the influence of band bending decreases with decreasing layer width. In addition, the photo-generation of holes in the InAs layer itself is decreased due to the decrease in layer thickness. Thus, the spatially *indirect* transitions across the hetero-interfaces become dominant.

The normal and inverted InAs/AlSb interface results in PL lines separated by 50 meV. The higher energy PL transition is assigned to the inverted interface. This assignment is supported by the reduced PL intensity for visible excitation due to the reduced penetration depth in comparison to IR excitation (see Fig. 4). Due to the hole capture in the underlying buffer layer, a space charge field arises (see Fig. 6), leading to a preferential accumulation of electrons at the bottom interface of the InAs layer, where the confinement energy of the triangular shaped potential is stronger. This leads to different PL transitions energies of the two interfaces.

3.4. Optical Anisotropy due to inequivalent Interfaces

The 100 nm layer exhibits a double peak structure of the spatially indirect PL. In the preceding chapter this has been attributed to the normal (AlSb on InAs) and inverted (InAs on AlSb) interface [14]. This assignment can be directly confirmed by polarized PL measurements: The PL shown in Fig. 5 has been recorded in the conventional geometry, i. e. excitation and emission normal to the {100} sample surface. A significant change of the two contributions depending on the polarization orientation is observed.

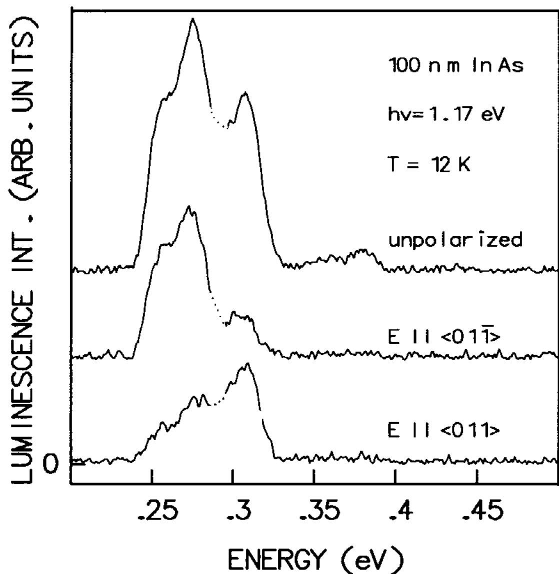

Fig. 5. Polarized PL of the 100 nm wide InAs layer. Excitation and emission was oriented normal to the {100} sample surface.

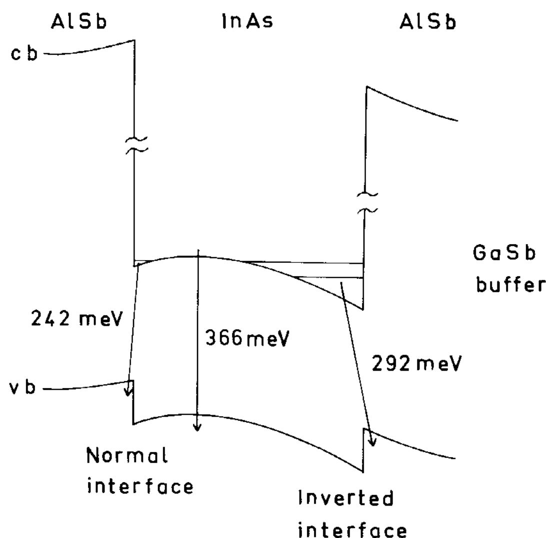

Fig. 6. Asymmetric potential shape of a wide InAs layer induced by space charge fields due to capture of photo-generated holes in the GaSb buffer layer. This leads to preferential electron accumulation at the bottom interface, where the confinement of the triangular shaped potential is stronger.

As outlined by Lavallard et al. [22] in type II SLs the degeneracy of the Γ_5 heavy exciton states is lifted and the two sublevels correspond to excitonic dipoles aligned along the [011] and [01$\bar{1}$] crystallographic axes. A perturbation of Γ_4 symmetry (which transforms like the unit vector $\mathbf{e}_{(100)}$ in growth direction) [23] together with the electron-hole exchange interaction has to be considered to describe the situation. The existence of the perturbation is related to the lowering from the D_{2d} symmetry of the ideal SL to the C_{2v} symmetry of the interfaces. Most likely the biaxial tension of the InAs layer is responsible for this perturbation. It is due to the existence of a shear strain located at the individual interface in the [011] and [01$\bar{1}$] directions, with opposite sign for normal and inverted interface [22].

The alignment of the excitonic dipoles along the crystallographic axes is illustrated in Fig. 7. In this figure the

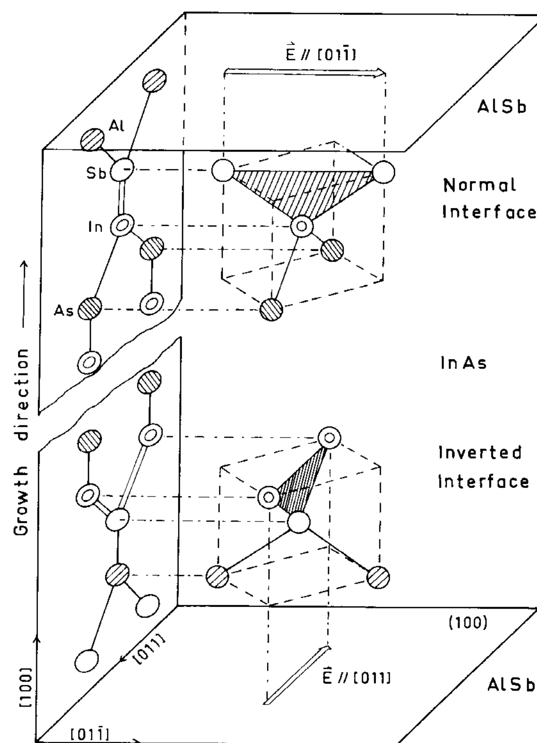

Fig. 7. Configuration of the tetrahedra which build up the normal (AlSb on InAs) and the inverted interface (InAs on AlSb) of a sample grown in [100] direction. The planes containing the InSb-like bonds of the heterointerfaces are drawn shaded. These planes are orthogonal to the (100) sample surface. The projection of these planes on the sample surface is parallel to the [01$\bar{1}$] direction for the normal interface and parallel to the [011] direction for the inverted interface. In addition the projection on a (01$\bar{1}$) plane is shown in the left part of the figure. In this part the projection of the InSb-like bonds is indicated with double lines.

tetrahedra which build up the InSb-like interfaces are shown. The planes containing the InSb-like bonds are drawn shaded. These planes are orthogonal to the (100) sample surface. The projection of these planes on the (100) sample surface is oriented in the $[01\bar{1}]$ direction for the normal interface, and in [011] direction for the inverted interface. Thus, if the contributions of the PL related to the two types of interface are not identical, a polarization dependence can be observed. Necessarily the type II exciton has to be localized at one of the two interfaces, otherwise differences due to the two types of interface cannot be expected. If the inverted interface grows structurally worse than the normal one, the creation of additional non-radiative centers will suppress the radiation of this interface and the PL intensity will be maximized with the polarization oriented in $[01\bar{1}]$ direction. In the present case the two contributions of the interfaces are spectrally separated due to the band bending induced by space charges (see Fig. 6), which facilitates the observation of this effect.

4. Summary

We have studied the photoluminescence of InAs/AlSb heterostructures and demonstrated the influence of the buffer layer sequence on the PL spectra. The relaxation of photo-generated holes into the underlying GaSb layers of the buffer system, leading to spatial separation of the excess carriers, is demonstrated to be a key mechanism. Calorimetric absorbance measurements show the spatially direct as well as the indirect contributions, spectrally separated by the value of the VBO. An increase of the thickness of the InSb-like IFs indeed leads to a red-shift of the PL as expected from the formation of a hole-attracting potential step at the IF. The PL of very wide InAs layers consists of both spatially-direct and spatially-indirect radiative transitions. Polarization dependent measurements allow to distinguish between the contributions of the normal and the inverted interface of the spatially indirect transitions.

Acknowledgment Helpful discussions with J. Wagner are gratefully acknowledged. The authors also thank K. Schwarz and G. Bihlmann for expert technical assistance.

REFERENCES

[1] A. G. Milnes and A. Y. Polyakov, Mater. Sci. and Eng. **B 18**, 237 (1993).

[2] A. Nakagawa, H. Kroemer, and J. H. English, Appl. Phys. Lett. **54**, 1893 (1989).

[3] H. Kroemer, C. Nguyen, B. Brar, J. Vac. Sci. Technol. B **10**, 1769 (1992); H. Kroemer,ibid **11**, 1354 (1993).

[4] G. Tuttle, H. Kroemer, and J. H. English J. Appl. Phys. **67**, 3032 (1990).

[5] S. Ideshita, A. Furukawa, Y. Mochizuki, and M. Mizuta, Appl. Phys. Lett. **60**, 2549 (1992)

[6] J. Shen, J. D. Dow, S. Y. Ren, S. Tehrani, and H. Goronkin, J. Appl. Phys. **73**, 8313 (1993).

[7] J. Scriba, S. Seitz, A. Wixforth, J. P. Kotthaus, G. Tuttle, J. H. English, and H. Kroemer Surf. Sci. **267**, 483 (1992).

[8] M. J. Yang, P. J. Lin-Chung, R. J. Wagner, J. R. Waterman, W. J. Moore, B. V. Shanabrook, Semicond. Sci. Technol. **8**, S129 (1993); M. J. Yang, P. J. Lin-Chung, B. V. Shanabrook, J. R. Waterman, R. J. Wagner, and W. J. Moore, Phys. Rev. B **47**, 1691 (1993).

[9] Y. Iwai, M. Yano, R. Hagiwara, and M. Inoue, Surf. Sci. **267**, 434 (1991).

[10] I. Sela, C. R. Bolognesi, L. A. Samoska, and H. Kroemer, Appl. Phys. Lett. **60**, 3283 (1992).

[11] J. Wagner, J. Schmitz, J. D. Ralston, and P. Koidl, Appl. Phys. Lett. **64**, 82 (1994).

[12] B. Brar, H. Kroemer, J. Ibbetson, and J.H.English, Appl. Phys. Lett. **62**, 3303 (1993).

[13] B. Brar, J. Ibbetson, H. Kroemer, and J.H.English, Appl. Phys. Lett. **64**, 3392 (1994).

[14] F. Fuchs, J. Schmitz, H. Obloh, J. D. Ralston, and P. Koidl, Appl. Phys. Lett. **64**, 1665 (1994).

[15] J. Schmitz, J. Wagner, H. Obloh, P. Koidl, and J. D. Ralston, J. Electron. Mater. 1993, (to be published).

[16] J. Wagner, J. Schmitz, M. Maier, J. D. Ralston, and P. Koidl, Solid-State Electron. **37**,1037 (1994).

[17] F. Fuchs, A. Lusson, J. Wagner, and P. Koidl, Proc. SPIE Vol. **1145**, 323. (1989).

[18] F. Fuchs, K. Kheng, P. Koidl, and K. Schwarz, Phys. Rev B **48**, 7884 (1993).

[19] F. Fuchs, K. Kheng, K. Schwarz, and P. Koidl, Semicond. Sci. Technol. **8**, S75 (1993).

[20] L. Podlowski, A. Hoffmann, and I. Broser, J. Crystal Growth **117**, 698 (1992).

[21] F. Fuchs, J. Schmitz, J. D. Ralston, and P. Koidl, Phys. Rev B **49**, 13638 (1994).

[22] P. Lavallard , C. Gourdon, and R. Planel, Superlattices and Microstructures **12**, 321 (1992).

[23] G. F. Koster, J. O. Dimmock, R. G. Wheeler, H. Statz in Properties of the 32 point groups, M. I. T. press, Cambridge, 1963.